Received: 21 April 2020 | Revised: 29 July 2020 | Accepted: 4 August 2020

DOI: 10.1111/cas.14616

ORIGINAL ARTICLE

Cancer Science WILEY

Lipid accumulation in macrophages confers protumorigenic polarization and immunity in gastric cancer

Qin Luo[1,2] | Naisheng Zheng[1] | Li Jiang[3] | Tingting Wang[1] | Peng Zhang[1] | Yi Liu[1] | Peiming Zheng[1,4] | Weiwei Wang[1] | Guohua Xie[1] | Lei Chen[5] | Dongdong Li[5] | Ping Dong[5] | Xiangliang Yuan[1] | Lisong Shen[1]

[1]Department of Clinical Laboratory, Xinhua Hospital, Shanghai Jiao Tong University School of Medicine, Shanghai, China

[2]Department of Clinical Laboratory, Affiliated Dongguan People's Hospital, Southern Medical University, Dongguan, China

[3]Department of Gynecology, Xinhua Hospital, Shanghai Jiao Tong University School of Medicine, Shanghai, China

[4]Department of Clinical Laboratory, Henan provincial people's Hospital, Zhengzhou, China

[5]Department of General Surgery, Xinhua Hospital, Shanghai Jiao Tong University School of Medicine, Shanghai, China

Correspondence
Lisong Shen and Xiangliang Yuan, Department of Clinical Laboratory, Xinhua Hospital, Shanghai Jiao Tong University School of Medicine, Shanghai, China.
Emails: lisongshen@hotmail.com or yuanxiangliang@gmail.com

Funding information
National Natural Science Foundation of China, Grant/Award Number: 81372641, 81402148, 81472244, 81672363 and 81772525; SMC - Morningstar Outstanding Young Teacher of Shanghai Jiao Tong University, Grant/Award Number: 15X100080007

Abstract

Heterotypic interactions between tumor cells and macrophages can enable tumor progression and hold potential for the development of therapeutic interventions. However, the communication between tumors and macrophages and its mechanism are poorly understood. Here, we find that tumor-associated macrophages (TAM) from tumor-bearing mice have high amounts of lipid as compared to macrophages from tumor-free mice. TAM also present high lipid content in clinical human gastric cancer patients. Functionally, TAM with high lipid levels are characterized by polarized M2-like profiling, and exhibit decreased phagocytic potency and upregulated programmed death ligand 1 (PD-L1) expression, blocking anti–tumor T cell responses to support their immunosuppressive function. Mechanistically, Kyoto Encyclopedia of Genes and Genomes (KEGG) pathway analysis identifies the specific PI3K pathway enriched within lipid-laid TAM. Lipid accumulation in TAM is mainly caused by increased uptake of extracellular lipids from tumor cells, which leads to the upregulated expression of gamma isoform of phosphoinositide 3-kinase (PI3K-γ) polarizing TAM to M2-like profiling. Correspondingly, a preclinical gastric cancer model is used to show pharmacological targeting of PI3K-γ in high-lipid TAM with a selective inhibitor, IPI549. IPI549 restores the functional activity of macrophages and substantially enhances the phagocytosis activity and promotes cytotoxic-T-cell-mediated tumor regression. Collectively, this symbiotic tumor-macrophage interplay provides a potential therapeutic target for gastric cancer patients through targeting PI3K-γ in lipid-laden TAM.

KEYWORDS

gastric cancer, lipid accumulation, polarization, tumor immunity, tumor-associated macrophages

Qin Luo, Naisheng Zheng, and Li Jiang contributed equally to this work.

This is an open access article under the terms of the Creative Commons Attribution-NonCommercial-NoDerivs License, which permits use and distribution in any medium, provided the original work is properly cited, the use is non-commercial and no modifications or adaptations are made.
© 2020 The Authors. *Cancer Science* published by John Wiley & Sons Australia, Ltd on behalf of Japanese Cancer Association

1 | INTRODUCTION

Gastric cancer (GC) is the second most frequent cause of cancer-related deaths worldwide.[1-3] Increasing evidence indicates that the tumor microenvironment plays a critical role in cancer progression and metastasis.[4] Tumor-associated macrophages (TAM) are key components of the tumor microenvironment that are recruited by tumor-derived signals and are correlated with poor prognosis in gastric cancer patients.[5-8] Animal and experimental studies have supported that TAM can provide a favorable microenvironment to promote tumor progression and metastasis.[5,9] In response to various microenvironment signals, macrophages can shift: M1-like and M2-like macrophages have distinct functional phenotypes, and while M1-like macrophage is involved in the pro–inflammatory response, the M2-like macrophage promotes the anti–inflammatory response.[10-12] It is generally accepted that TAM display the M2-polarized phenotype and are a critical player in the tumor microenvironment.[5,13,14]

Recent evidence has shown that various tumor-derived factors regulate the polarization and function of macrophages.[15] However, the detailed molecular mechanism by which these factors regulate TAM remains unknown. Several reports have revealed the importance of lipids in the function of immunosuppressive myeloid cells in cancer and chronic inflammatory conditions.[16-18] In addition, the important role of excessive lipid accumulation in macrophages has been well established in the development of atherosclerosis.[19,20] However, the exact biological role of lipid accumulation in TAM of gastric cancer remains to be explored.

In this study, we characterized the phenotype of lipid-laid TAM and explored the mechanism of metabolic reprogramming and functional polarization of TAM in gastric cancer. Based on this, we provide a potentially attractive therapeutic target of lipid-accumulated TAM in gastric cancer. Our data demonstrated that gastric cancer cells have a significant impact on TAM through lipid accumulation, which indicates specific signaling pathways, therapeutic and diagnostic approaches, as well as prognostic biomarkers.

2 | MATERIALS AND METHODS

2.1 | Animal model

Female 615 mice (6-8 weeks old) were purchased from the Institute of Hematology of the Chinese Academy of Medical Sciences (Tianjin, China). For the MFC-bearing tumor model, the PI3K-γ inhibitor drug IPI-549 (Cat. 26416, Cayman Chemical) was administered by oral gavage every day at a concentration of 15 mg/kg. Treatment was initiated on day 5 and ended on day 15 post–tumor implant. Tumor volume was calculated using the formula $V = (L \times W^2)/2$. The animal experiment was approved by the Animal Ethical and Experimental Committee of Xinhua Hospital, Shanghai Jiao Tong University School of Medicine.

2.2 | Patient samples

Fresh gastric tumor tissues, ascites, and autologous peripheral blood were obtained from patients with gastric cancer who underwent treatment at Xinhua Hospital, Shanghai Jiao Tong University School of Medicine, China. The use of clinical samples was approved and informed consent forms were signed by each patient before participation.

2.3 | Cell culture

The mouse gastric cancer cell line MFC was obtained from the Cell Bank of Type Culture Collection of Chinese Academy of Sciences and cultured in DMEM: F12 (Gibco) containing 10% FBS with 100 U/mL penicillin and 100 μg/mL streptomycin in 5% CO_2 at 37°C. The human gastric cancer cell line AGS (CRL-1739, ATCC), the murine breast cancer cell line 4T1 (CRL-2539, ATCC), the murine colon carcinoma cell line MC38, and the human gastric cancer cell line MGC-803 (Chinese Academy of Sciences Cell Bank) were grown in monolayer cultures in the recommended medium. All cultured cells were tested to confirm they were negative for mycoplasma contamination.

2.4 | Bone marrow-derived macrophages and tumor-associated macrophages

Murine bone marrow-derived macrophages (BMDM) were generated from the bone marrow of 615 mice and cultured for 6 days with 50 ng/mL M-CSF (R&D Systems). The polarization of macrophages was performed as previously described.[21] For the inhibition assay, IPI-549 (Selleck, S8330) 1 μmo/L, PI3Kγ inhibitors, were used and incubated with macrophages for 1 hour before polarizing stimuli. Peritoneal macrophages (PM) were collected from the peritoneal cavity 96 h after i.p. injection of 3% thioglycollate. Mouse MFC cells (5×10^5) were injected into the abdominal cavities of 615 mice in 100 μL of PBS and allowed to grow for 10-15 days. Ascites was collected for TAM separation.

2.5 | Tumor supernatant preparation and collection

MFC tumor explants were removed after the mice were killed. Tumors tissues were digested and pressed through a 70-μm nylon filter. After centrifuging, cells were cultured overnight in RPMI 1640 complete medium. The cell-free supernatant was collected to prepare tumor explant supernatant (TES). MFC cells were grown in the DMEM-complete medium. After 1 day, the medium was recovered and filtered to prepare the tumor-conditioned medium (TCM).

2.6 | Lipid staining

The sorted TAM or in vitro-treated macrophages were fixed with 4% paraformaldehyde, stained with oil red O (Sangon Biotech) for 1 hour at room temperature (RT) according to the manufacturer's protocols, and then imaged with light microscopy. For BODIPY 493/503 staining, the slides were stained with BODIPY 493/503 (Thermo Fisher Scientific) at 0.5ug/mL for 15 min at RT, as previously described.[22] Slides were imaged with immunofluorescence microscopy.

2.7 | Flow cytometry assay

Single cells were generated from mouse tumors or spleens, and then pre–incubated with the anti–CD16/32 monoclonal antibody (BD Biosciences) to block nonspecific binding. Appropriate dilutions of various combinations of fluorescently-labeled antibodies were used and are listed in Table S1. BODIPY 493/503 staining was performed as previously described.[22] For sorting cells, the gate was set to discriminate TAM with normal lipid content (TAM-NL) versus TAM with higher lipid content (TAM-HL) in the tumor-bearing host using the fluorescence of naïve macrophages as the background defining normal lipid levels. For the cell cycle assay, the cells were stained with propidium iodide (PI, 20 μg/mL). Apoptosis was measured using the FITC Annexin V Apoptosis Detection Kit I (BD) following the manufacturer's protocol. All flow experiments were performed using FACS Aria II machines (BD).

2.8 | Phagocytosis assay

The phagocytosis assay was performed with pHrodo Red *Staphylococcus aureus* bioparticles (Thermo Fisher Scientific). Sorted macrophages were plated at 5×10^5 cells/well into six-well tissue culture plates. A single vial of lyophilized *Staphylococcus aureus* bioparticles labeled with pHrodo Red was resuspended in 2 mL of Hank's balanced salt solution with 5% FBS. Bioparticles were added to a confluent monolayer of cells at a ratio of 1 vial per 2×10^6 cells, as per the manufacturer's instructions. All cells were incubated with bioparticles for 4 hours and then processed for FACS analysis. To quantify the phagocytosis, the ratio of the Red^+ macrophages to the total macrophages was evaluated and analyzed using FlowJo (Tree Star) and was normalized as indicated in the figure legends.

2.9 | T cell proliferation assay

Spleens from the 615 female mice were isolated and generated to a single-cell suspension. After red blood cell lysis, $CD8^+$ cells were purified using anti–CD8 microbeads (Miltenyi Biotech) following the manufacturer's instructions, and then purified $CD8^+$ T cells were labeled with 5 μmol/L carboxyfluorescein succinimidyl ester (CFSE) (#423801, BioLegend) in PBS for 6 min at 37°C. The CFSE-labeled $CD8^+$ T cells were then plated in complete RPMI 1640 media supplemented with 0.05 M β-mercaptoethanol onto 96-well plates coated with 2 μg/mL anti–CD3 (clone 1454-2C11, BioLegend) and 1 μg/mL anti–CD28 (clone 37N, BioLegend) antibodies. Sorted TAM-NL or TAM-HL cells were added in indicated ratios and were incubated at 37°C. For Ab blocking assay, anti–IgG2a Ab or anti–PD1 Ab (10 μg/mL) was added in the coculture system. After 96 hours, cells were harvested and T cell proliferation was measured by CFSE-dilution assay in the gated $CD8^+$ T cells by flow cytometry (BD Canto II, BD Biosciences).

2.10 | Lipidomics analysis

For lipidomic analysis, TES of MFC cells derived from MFC-bearing mice were harvested. Macrophages were treated with control medium (n = 5) or 30% TES (n = 5) for 48 hours and then harvested for lipidomic analysis. Lipids of samples were extracted and analyzed at Shanghai Applied Protein Technology. LC/ESI-MS analysis of lipids was performed on a UPLC-Q-Exactive Orbitrap MS system and untargeted relative quantitative lipidomics analysis was conducted.

2.11 | Kyoto Encyclopedia of Genes and Genomes enrichment analysis

Total RNA was extracted and reverse-transcribed into cDNA to generate indexed Illumina library, followed by sequencing. Gene set enrichment analysis (GSEA) was performed based on differentially expressed genes in different clusters. Upregulated and downregulated sets of genes were ranked and normalized to log10 fold change between TAM and naïve macrophages, and each gene set was assessed for enrichment using the Kyoto Encyclopedia of Genes and Genomes (KEGG) annotations. For validating gene expression, target gene-specific primers were used and described in Table S2. The RT-PCR analysis was performed with 7900 HT Real-Time PCR with SYBR Premix Ex Taq (Takara).

2.12 | Western blot

Total protein was isolated from macrophages treated with PBS, 30% tumor cells culture media, or lipid mixture for 48 hours. Proteins were detected by incubation with appropriate dilutions of primary antibodies (listed in Table S3), washed and incubated with secondary antibodies, and detected after incubation with a chemiluminescent substrate.

2.13 | Transwell migration and invasion assay

MFC cells were seeded in transwell chambers (Corning) with 8-um-sized pores at 30 000 cells per well. MFC cells were

cultured in DMEM: F12 containing 1% FBS, and the differently treated macrophages were added to the bottom plate with 10% FBS. For the transwell invasion assay, MFC cells were seeded on the upper transwell chambers precoated with ECM Matrix gel solution. After 24 hours, the number of MFC cells that had passed through the membrane was counted using Image J (NIH). Five random fields per chamber were captured and statistically analyzed.

2.14 | Statistical analyses

Statistical analyses were performed with GraphPad PRISM 8.0 software. Variables were compared between two independent groups with the Mann–Whitney test, and two-way ANOVA if there were more than two groups. $P < 0.05$ was considered statistically significant.

3 | RESULTS

3.1 | Lipid accumulation in tumor-associated macrophages

To assess the amount of lipids in TAM, we used an immunocompetent syngeneic setting with a murine gastric cancer MFC model. Immunofluorescence microscopy of TAM from dissociated tumors 2 weeks after engraftment into mice revealed more BODIPY 493/503 fluorescence in TAM than in their control counterparts (Figure 1A, B; Figure S1). Oil red staining of sorted TAM confirmed abundant lipid

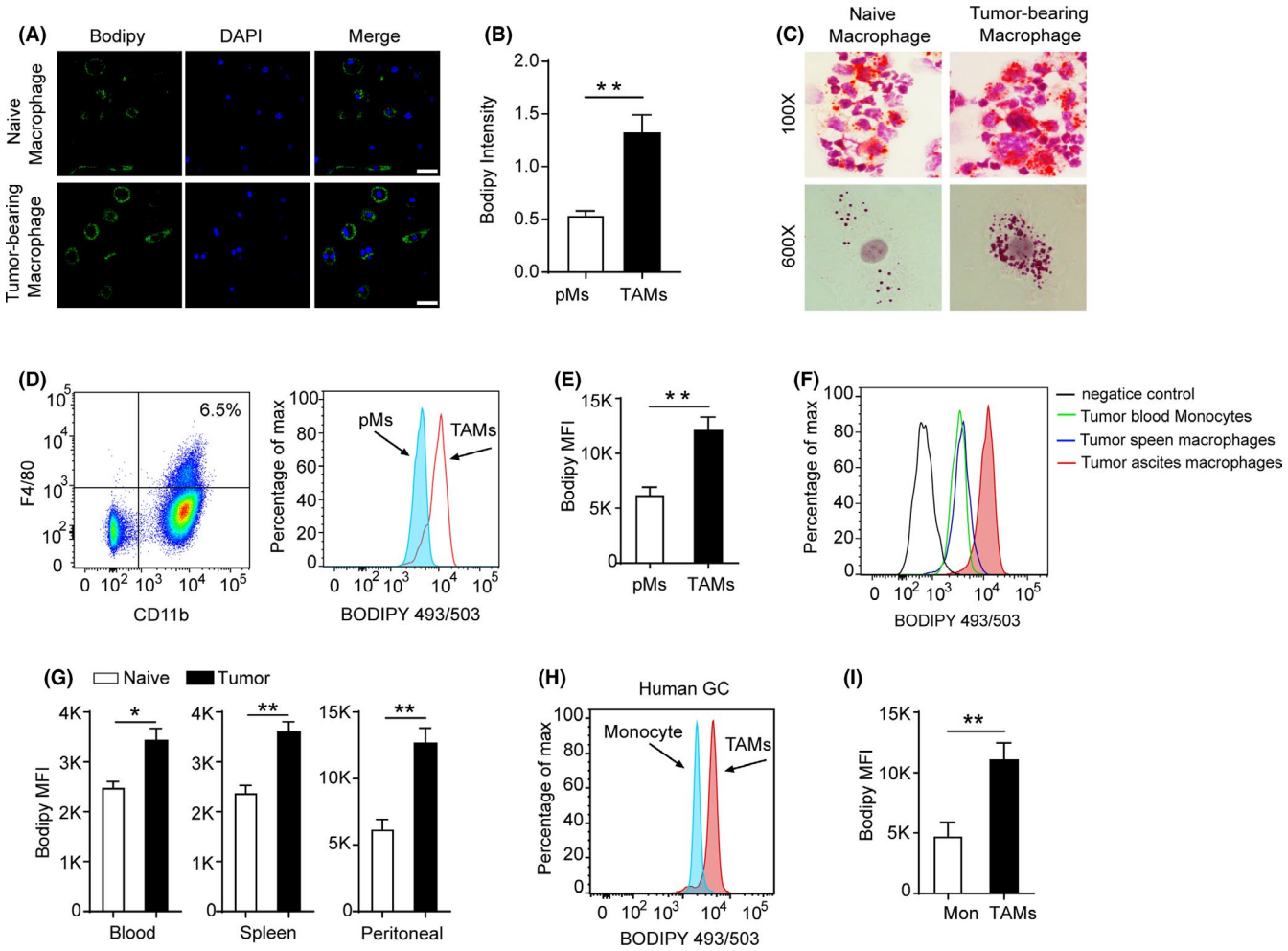

FIGURE 1 Lipid accumulation in mouse and human tumor-associated macrophages (TAM). A, Immunofluorescence images of F4/80$^+$ macrophages from the peritoneal of naïve mice and the ascites of MFC tumor-bearing mice staining with BODIPY 493/503. n = 3. Scale bar, 20 μm. Green, BODIPY 493/503; blue, DAPI. B, Immunofluorescence intensity of BODIPY 493/503 in F4/80$^+$ peritoneal macrophages (pMs) or TAM was measured. C, neutral lipids were stained with oil red O and counterstained with hematoxylin. D, A typical example of the analysis of lipid level in F4/80$^+$ macrophages from peritoneal of control (blue) or ascites of MFC tumor-bearing mice (red) by FACS. E, Geometric mean fluorescence intensity (MFI) of BODIPY 493/503 was measured by FACS. n = 5. F, Lipid level in F4/80$^+$ macrophages from blood, spleen, and ascites in MFC tumor-bearing mice or WT mice. n = 3. G, Lipid levels in macrophages from naïve or MFC tumor-bearing mice collected on week 2 after tumor inoculation. H, Typical FACS analysis of BODIPY 493/503 in TAM from the individual with gastric cancer (GC). I, Cumulative results of lipid levels in TAM from individuals with GC

accumulation in TAM (Figure 1C). By flow cytometry, macrophages were identified as CD11b$^+$F4/80$^+$ cells (Figure 1D). Significantly increased lipid content was also observed in TAM, whereas that in peritoneal naïve macrophage was lower (Figure 1D, E), further confirming the lipid accumulation in TAM. In tumor-bearing mice, TAM isolated from tumors had higher levels of lipids than from the spleen (Figure 1F). TAM in the spleen, the peritoneal cavity, and the blood from tumor-bearing mice had higher levels of lipids than macrophages from control mice (Figure 1G). This is a consistent observation in TAM from mouse breast cancer 4T1 and colon carcinoma MC38 tumor models (Figure S2A, B, C). Based on this finding in mice, we next explored human TAM from patients with gastric cancer. Upon profiling the TAM in human gastric cancer samples, in line with mice, TAM in patients with gastric cancer had more elevated lipid content than monocyte-derived macrophages (Figure 1H, I). Thus, our data strongly indicate that there is enriched lipid content in TAM from mouse tumor models or subjects with gastric cancer.

3.2 | Characterization of lipid-laden tumor-associated macrophages by M2-like status

To characterize the phenotype of lipid-accumulated TAM, TAM with different lipid content from MFC tumor-bearing mice were sorted using the gating strategy set around lipid levels in control macrophages (Figure 2A). By flow cytometry, we detected two populations of F4/80$^+$ TAM from tumor-bearing mice. One population, termed TAM with normal lipid content (TAM-NL), represented 20%-30% of cells and had a similar level of fluorescence to naïve macrophages (Figure 2A, B). The other population (60%-80% of cells), referred to as TAM with high lipid content (TAM-HL) (Figure 2B), had a higher level than that in control macrophages (Figure 2C). Flow cytometry analysis of typical TAM markers showed that TAM-NL and TAM-HL from MFC tumors expressed equivalent levels of CD11b and F4/80, but TAM-HL expressed more of the M2-associated scavenger receptor CD206, less M1-associated maker MHC class II, and

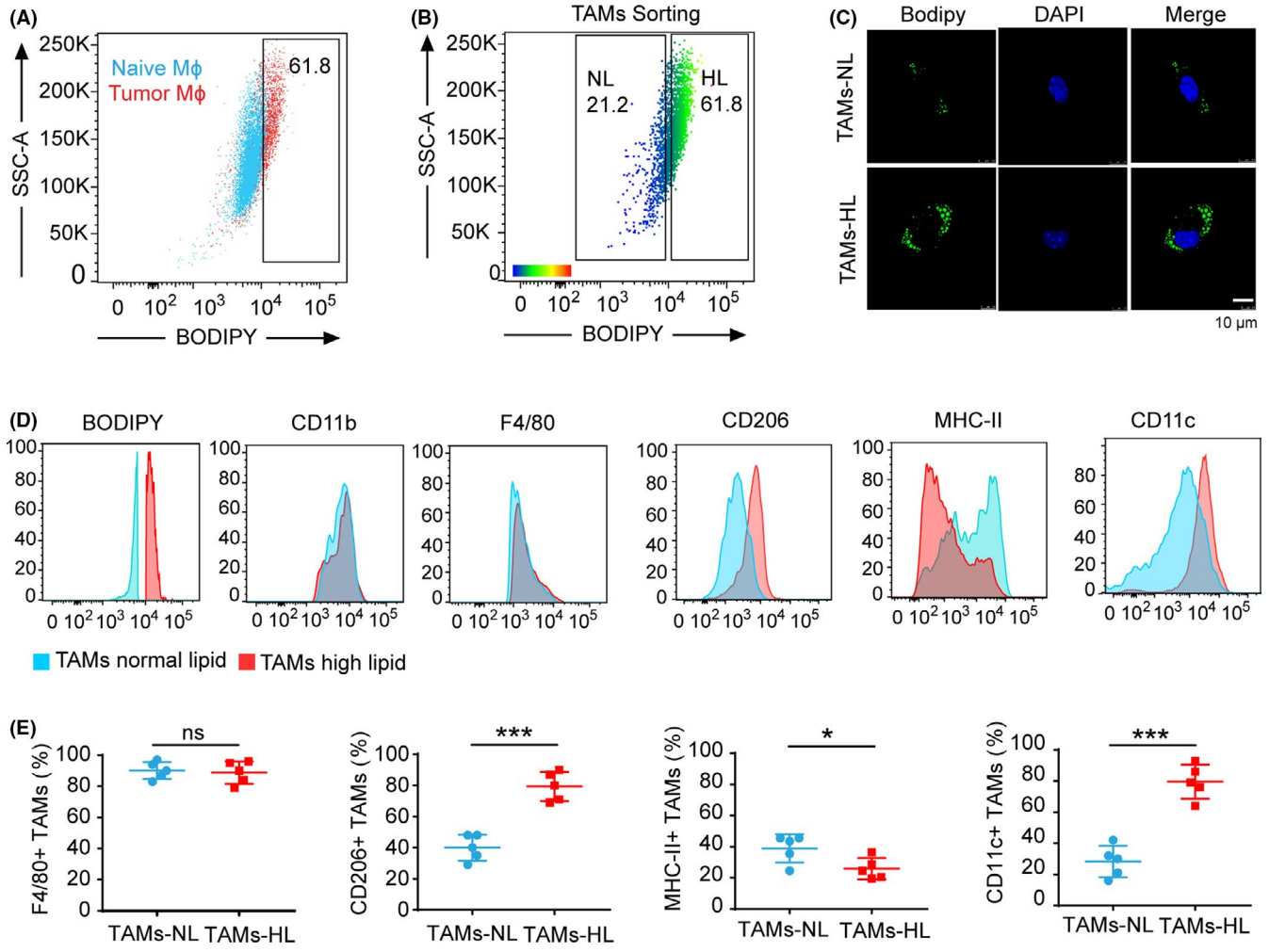

FIGURE 2 Characterization of lipid-accumulated tumor-associated macrophages (TAM). A, Dot plot shows the overlay of naïve macrophages and TAM based on different lipid levels, setting the cutoff of normal lipid levels in the macrophage. Blue, naïve mouse; red, tumor-bearing mouse. B, Examples of gates set for the sort of F4/80 + TAM with normal lipid (NL) and high lipid (HL) content isolated from MFC tumor-bearing mice. C, Immunofluorescence analysis of BODIPY 493/503 in sorted F4/80$^+$ TAM with different lipid levels. Scale bar, 10 μm. D. Representative flow cytometry histograms showing expression of typical TAM markers in TAM-NL versus HL from MFC tumors. n = 5. E, Quantification analysis of TAM markers in TAM-NL versus TAM-HL subsets from MFC tumors. n = 5

more CD11c (Figure 2D, E). These data suggest that TAM with different lipid content have varying phenotypes. Almost all TAM with high lipid content express an M2-like surface profile.

3.3 | Lipid-laden tumor-associated macrophages exert tumor-promoting functional activity

Based on the different polarized status of TAM-NL and TAM-HL, we were curious about the functional activity of TAM with various lipid contents. We sorted TAM-NL and TAM-HL from MFC tumors and performed a phagocytosis assay using RED + *Staphylococcus aureus* bioparticles. TAM-HL displayed a reduced degree of phagocytosis of *S. aureus* bioparticles relative to the TAM-NL (Figure 3A–C), suggesting a reduced capacity for phagocytosis in lipid-accumulated TAM. Next, transwell analysis showed that TAM-HL promoted significantly more MFC tumor cell migration than TAM-NL (Figure 3D, E). Currently, the programmed death-1 PD1/programmed death ligand 1 (PD-L1) pathway blockade is a promising therapy for treating multiple cancers, including gastric cancer. Macrophages expressing PD-L1 may shape and predict the clinical efficacy of PD-L1/PD-1 blockade. We found that TAM-HL exhibited higher PD-L1 intensity than TAM-NL (Figure 3F), but there was no significant change in PD-L2 between TAM-HL and TAM-NL (Figure S3A), which means that TAM-HL displays the capacity of anti–tumor immunity by elevated PD-L1. We subsequently tested the effect of TAM with various lipid contents on T cell proliferation. TAM from control mice and TAM-NL from MFC tumor-bearing mice had similar effects, whereas TAM-HL substantially reduced the allogeneic T cell proliferation (Figure 3G, H); this

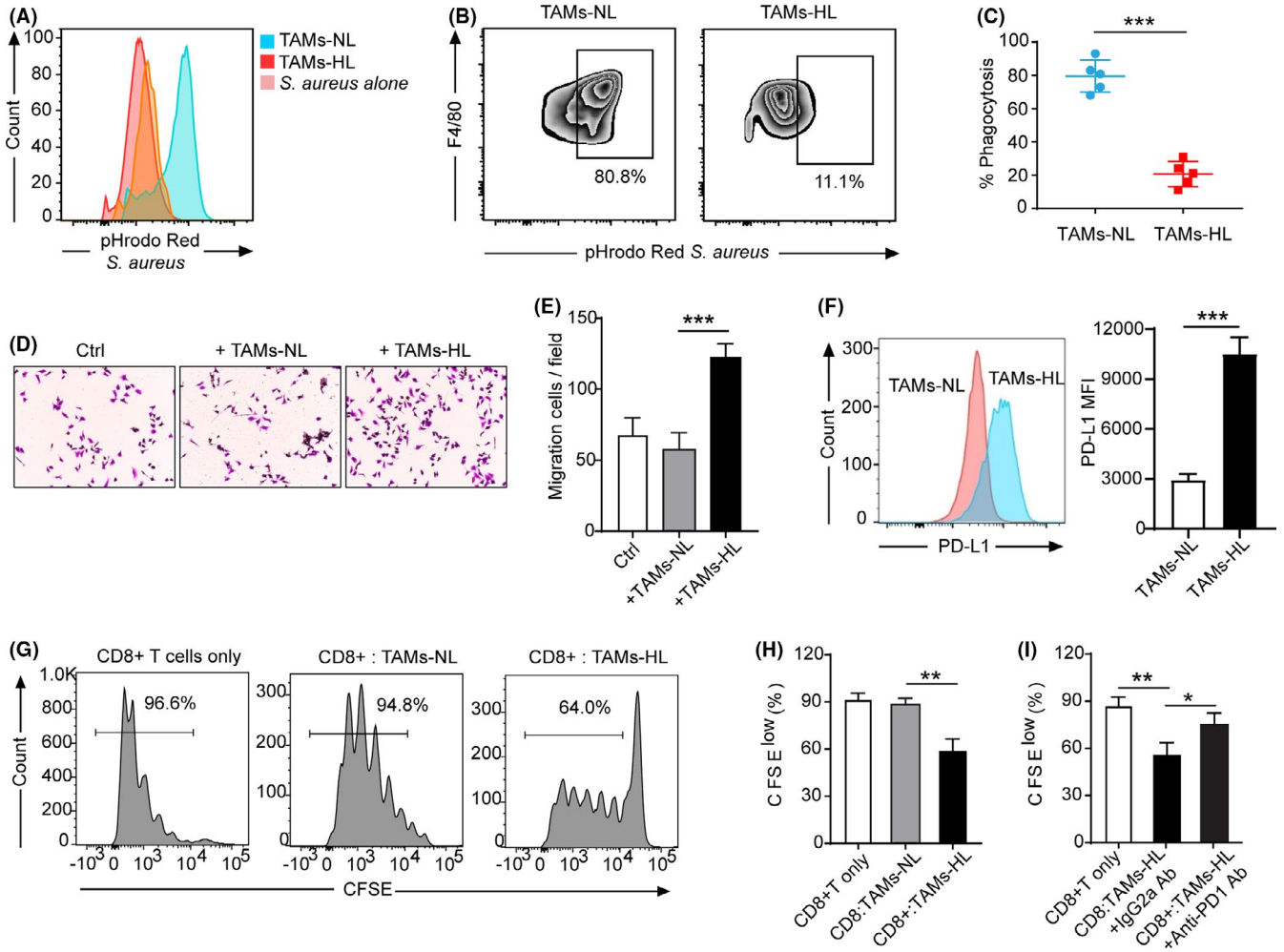

FIGURE 3 The pro–tumor functional activity of lipid-accumulated tumor-associated macrophages (TAM). A, Representative histogram showing the difference in RED fluorescence of TAM-normal lipid (NL) versus TAM-high lipid (HL) by phagocytosis assay. B, Representative histograms showing the flow cytometry gating strategy for phagocytosis by TAM-NL and TAM-HL. RED^{high} TAM were considered to be phagocytosing. C, Analysis of phagocytosis shows that TAM-HL phagocytosed significantly less than TAM-NL. n = 5. ***$P < 0.001$. D, E, Migration assay of MFC cells cocultured with sorted TAM-NL or TAM-HL after 24h incubation. Representative images (D) and quantification of migration cells (E) are shown. ***$P < 0.001$. F, Programmed death ligand 1 (PD-L1) expression level of TAM-NL and TAM-HL from MFC tumor-bearing mice. G, H, I, Representative histograms of $CD8^+$ T cell proliferation at $CD8^+$ T cells to TAM ratio 1:1 (G) and quantification of $CD8^+$ T cell proliferation in indicated condition using carboxyfluorescein succinimidyl ester (CFSE) dilution assay (H, I) (n = 3). *$P < 0.05$. **$P < 0.01$

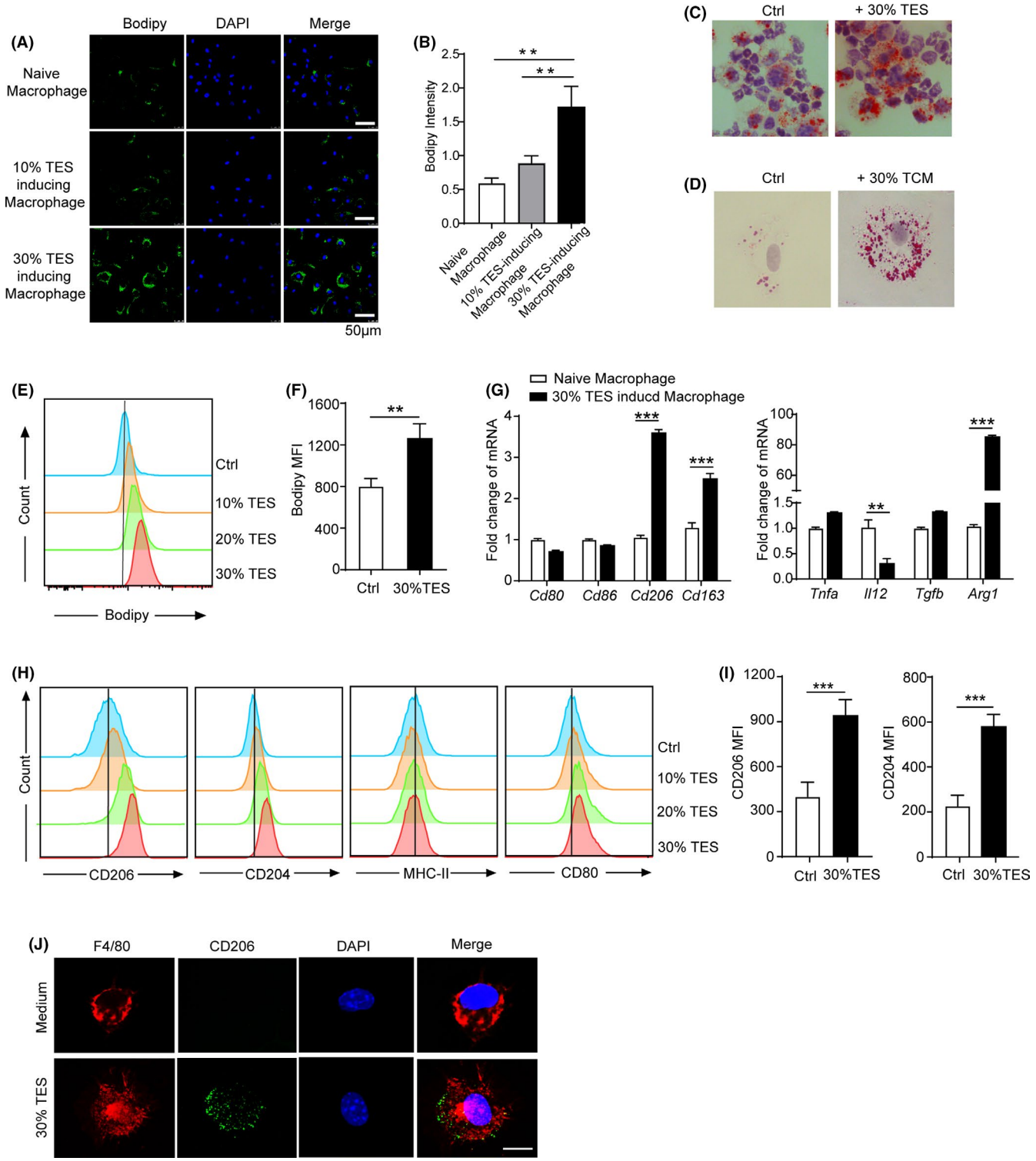

FIGURE 4 Tumor explant supernatants induce lipid accumulation to generate cancer-supporting M2 macrophages. A, Immunofluorescence images of lipid level in naïve peritoneal macrophages cultured with 10%, 30% MFC-tumor explant supernatant (TES) for 24 h. B, Quantification of the intensity of BODIPY 493/503 by ImageJ. n = 5. C, D, Oil red O staining the lipid content in macrophage cultured with 30% MFC-TES (Mag. 100×) (C) or with 30% MFC-tumor-conditioned medium (TCM) for 24 h (Mag. 600×) (D). E, F, Representative histogram showing lipid level (E) and quantification of the intensity (F) in naïve peritoneal macrophages cultured with indicated concentrations of MFC-TES for 24 h. G, mRNA expression of the indicated typical M1 and M2 markers in macrophage cultured with control medium or 30% TCM for 48 h. The results are normalized to β-actin. H, I, Representative histogram (H) and quantification (I) show that 30% of MFC-TES-treated macrophages have higher expression of CD206 and CD204 than naïve macrophages. *n* = 5; three experimental repeats. J, Immunofluorescence images of TCM-treated macrophage. Scale bar, 20 μm. Red, F4/80; green, CD206; blue, DAPI

suppressive effect was partly mediated by elevated PD-L1 expression in TAM-HL (Figure 3I).

3.4 | Tumor cells induce lipid accumulation to generate tumor-supporting M2-like macrophages

Depending on the environmental stimuli, TAM are polarized to an inflammatory M1-like *or pro–tumor* M2-like state.[13,23] We hypothesized that tumor-derived signals induce the lipid accumulation in macrophage, and then educate macrophages to reach a tumor-promoting state that is characterized by an M2-like profile. To test this hypothesis, we incubated in vitro-generated macrophages with TES from MFC gastric cancer-bearing mice. Thirty percent TES resulted in a more than threefold increase in the lipid level of macrophages (Figure 4A, B). Oil red staining and flow cytometry analysis confirmed this significantly increased lipid accumulation in macrophages treated with TES or TCM (Figure 4C, D, E). Similar results were obtained in experiments with in vitro BM-derived macrophage cultured with TCM (Figure S3B). We further tested whether TES or TCM-induced lipid accumulation can polarize macrophage to M2-like profile. The expression of prototypic M2 markers (*CD206*, *CD163*, *TGFβ*, *Arg-1*) were increased, while M1 markers (*IL-12*, *CD80*) were reduced in TES-treated macrophages (Figure 4F). Furthermore, relative mRNA expression of M1 and M2 biomarkers are correlated with a high lipid accumulation of these cells. We also detected elevated CD206 expression in macrophage cultured with TES (Figure 4H, I) or TCM (Figure S3C). We confirmed the co–expression of CD206 and F4/80 on TES-induced macrophages by immunofluorescence microscopy (Figure 4J).

3.5 | Tumor-derived lipids or exogenous lipids are sufficient to induce M2 polarization of macrophage

Next, we sought to determine which factor from the tumor is critical to promote the lipid accumulation in the macrophage. Given that the tumor microenvironment is rich in lipids, including fatty acids and triacylglycerols,[17] we are curious whether the tumor cells secrete lipids for uptake by TAM. To test this, we performed the lipidomic profiling of MFC-TES derived from MFC-bearing mice collected at 15 days after tumor implantation, and we confirmed the high enrichment of lipids such as triacylglycerols (TG) in TES (Figure S4A, B), meaning that cancer cells secrete the lipids to cause comparable upregulation of lipids in TAM. To further confirm the lipid accumulation in TAM due to tumor-derived lipids, the lipidomic analysis revealed that TAM generated in the presence of TES had an almost 10-fold higher level of TG than TAM generated in the control culture medium (Figure S4C, D). There was an increase in the level of all molecular species of TG, but we observed no changes in the level of cholesteryl esters in these TAM (Figure S4E).

To test the direct effect of lipids on the characterization of macrophages, we used exogenous lipid mixture to treat macrophages. Using immunofluorescence and oil red staining, clear consistent data

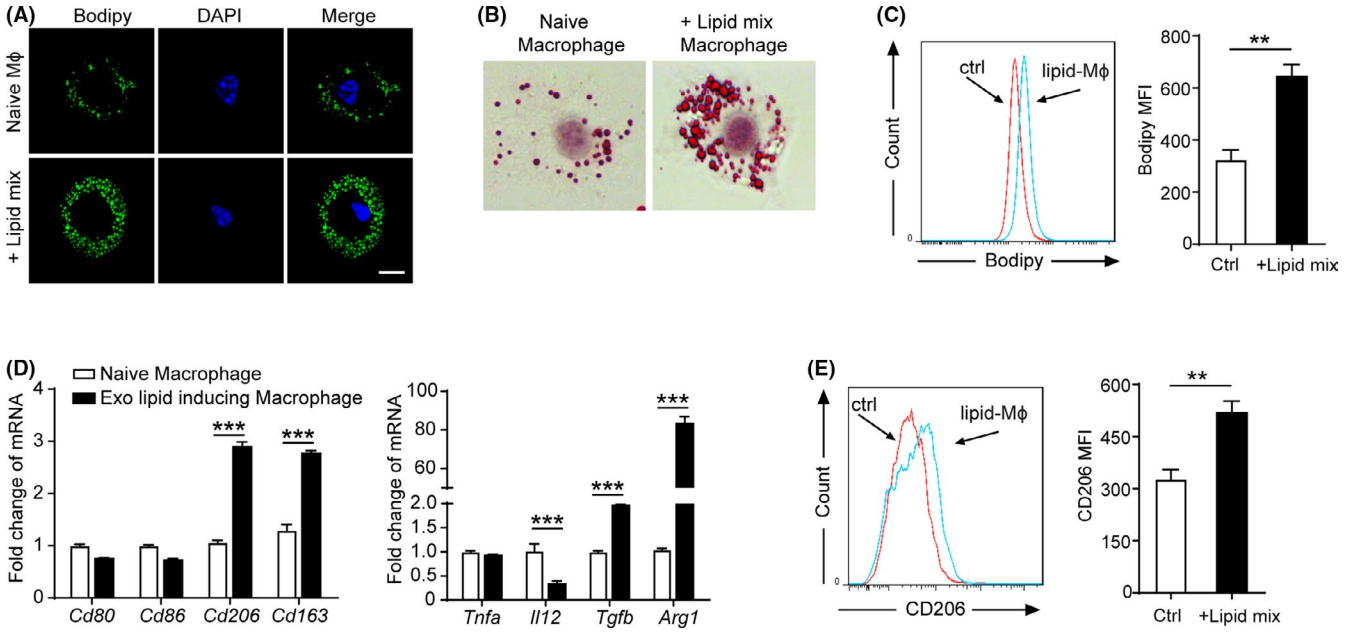

FIGURE 5 Exogenous lipid mixture is sufficient to induce M2 polarization of macrophage. A, Immunofluorescence images of lipid level in naïve peritoneal macrophages cultured in the presence of vehicle or 2 μg/mL exo-lipid mixtures for 24 h. B, Oil red O staining the lipid content in macrophage treated with 2 μg/mL exo-lipid mixtures for 24 h (magnification 600×). C, Representative histogram showing lipid level (left panel) and quantification of lipid content (right panel) in naïve peritoneal macrophages treated with 2 μg/mL exo-lipid mixtures or control medium for 24 h. D, mRNA expression of the indicated typical M1/M2 markers and typical cytokine genes in macrophage cultured for 48 h with the indicated condition. E, Representative histogram (left panel) and quantification (right panel) show that lipid mixture-treated macrophages have higher expression of CD206 than control. $n = 5$; three experimental repeats

showed that exogenous lipids caused comparable upregulation of lipids in macrophage (Figure 5A, B). Flow cytometry analysis also confirmed the elevated lipid in macrophage with the stimulation of exogenous lipid mixture (Figure 5C). Next, we asked whether exogenous lipid induced-macrophage has an M2-like phenotype. The mRNA level of M1/M2 markers showed that similarly to the induction by tumor-conditioned media, exogenous lipid mixture induced the expression of prototypic M2 markers after treatment with lipid for 48 hours (Figure 5D). The magnitude of CD206 induction in macrophages correlated with the amount of lipid in the cultured media (Figure 5E).

3.6 | Lipid accumulation polarizes pro–tumor M2-like macrophages via PI3K-γ

To explore the molecular mechanism of lipid-accumulated TAM inducing the protumor function, we performed GSEA on TAM and naïve macrophages in an MFC gastric cancer model. Of note, GSEA indicated significant enrichment of the "KEGG_PI3K-AKT signaling pathway" and "KEGG_Glycerophophalipid metabolism" in TAM of MFC-bearing mice model (Figure 6A). Recently, PI3K-γ has been established as controlling the TAM switch by directly regulating macrophage polarization.[24,25] Therefore, we hypothesized that the PI3K

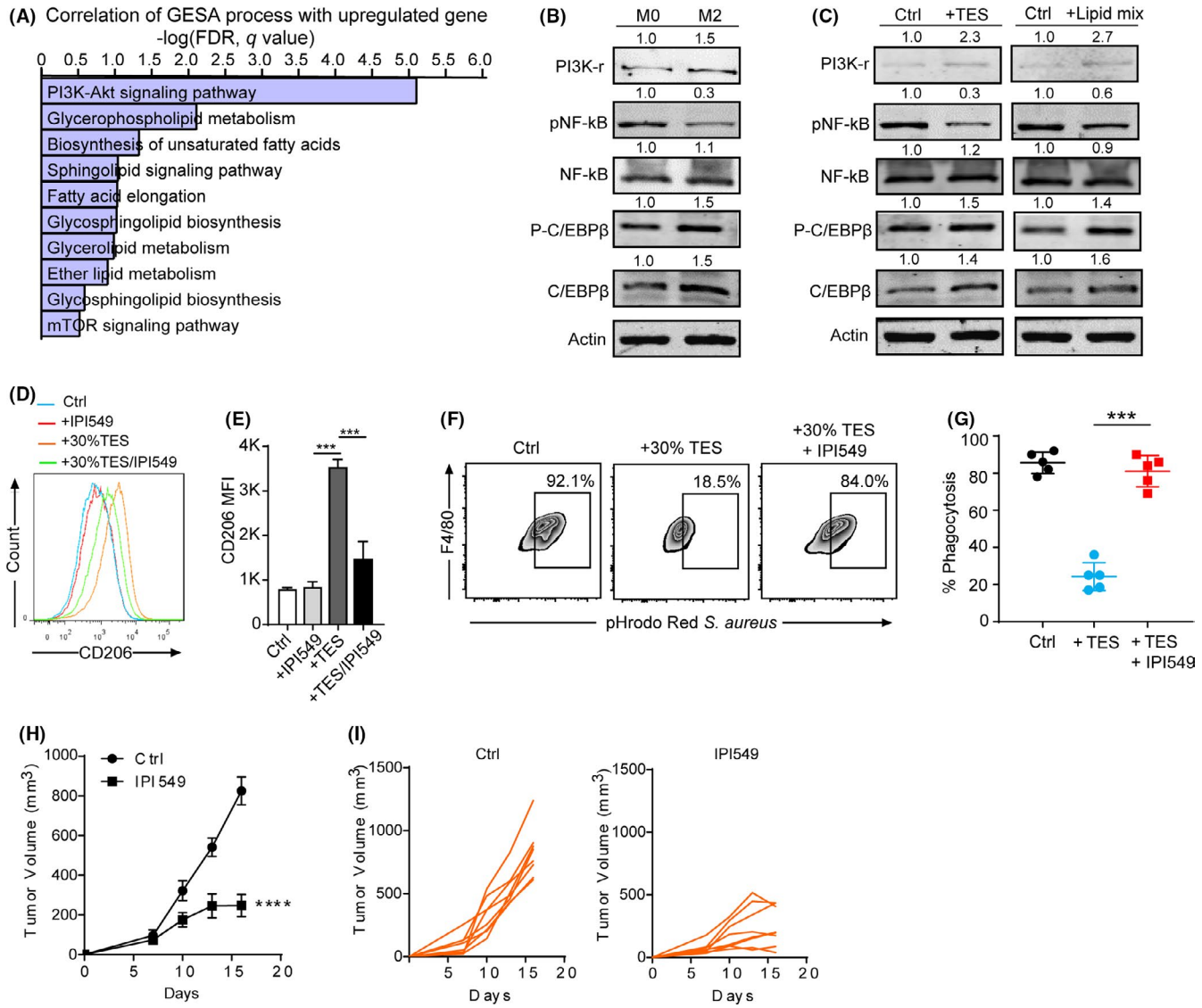

FIGURE 6 Lipid accumulation polarizes macrophages to an M2-like state that is critical for pro–tumor potential via PI3K-γ. A, The top enrichment of the Kyoto Encyclopedia of Genes and Genomes (KEGG) gene set in tumor-associated macrophages (TAM) from the MFC-bearing tumor model is shown. B, WB immunoblotting of indicated proteins in M0 and M2 macrophages. C, Immunoblotting in macrophages treated with 30% MFC-tumor explant supernatant (TES) and 2 μg/mL exo-lipid mixtures for 48 h. D, E, Representative overlay histogram (D) and quantification (E) showing PI3K-γ inhibitor (IPI549) reverse the high expression of CD206 in MFC-TES-treated macrophages. $n = 5$; three experimental repeats. Data are mean + SEM; $^{***}P < 0.001$. F, Representative histograms showing the phagocytosis by macrophage treated with 30% MFC-TES and/or IPI549. G, Analysis of phagocytosis in macrophage treated with 30% MFC-TES and/or IPI549. $n = 5$. $^{***}P < 0.001$. H, Mean tumor volume of MFC murine gastric cancer in 615 mice administered with IPI-549 versus vehicle-treatment ($n = 8$). Data are mean ± SEM; $^{****}P < 0.0001$. I, Individual tumor volumes of intradermal MFC implants in mice treated with IPI-549 or vehicle ($n = 8$)

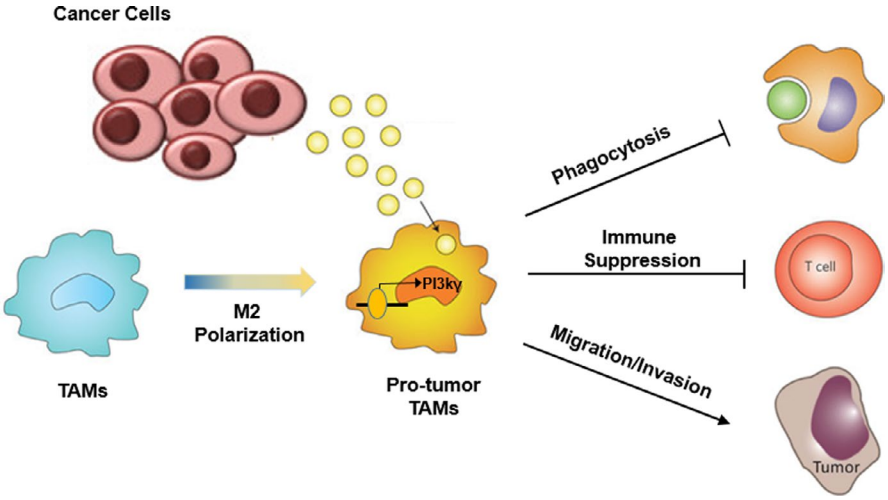

FIGURE 7 Schema of protumorigenic characteristics of lipid-accumulated macrophages. Tumor-associated macrophages (TAM) with high lipid content exhibit the protumorigenic characteristics with decreased phagocytosis and impaired anti–tumor immunity. Mechanically, tumor-derived lipids induce TAM to M2-like polarization via the PI3K-γ signaling pathway and pharmaceutical targeting PI3K-γ overcomes the protumoral TAM function

signaling pathway was involved in lipid-accumulated TAM. To test this, we analyzed protein expression in primary macrophages stimulated with anti–inflammatory (IL4 and IL-13) conditioned medium in vitro. Consistently, anti–inflammatory stimuli induced expression of PI3K-γ, and inhibited NF-κB p65–RelA phosphorylation and simultaneously increased C/EBPβ and phosphorylation (Figure 6B), which confirms that PI3K-γ controls the macrophage polarization switch. We next investigated whether MFC-TES and exogenous lipid mixture induced elevated expression of PI3K-γ, and inhibited NF-κB p65 phosphorylation and increased C/EBPβ (Figure 6C). Then, we examined whether inhibition of PI3K-γ rescued M2-like phenotype in macrophage stimulated with TES or lipid mixture. Ablation of PI3K-γ by IPI-549, a specific PI3K-γ inhibitor, suppressed the upregulated CD206 expression, which was an M2-like macrophage marker and can be induced by TES or exogenous lipid mixture, while IPI-549 had no effect on CD206 expression (Figure 6D, E).

3.7 | Targeting PI3K-γ reverses the protumor function of lipid-accumulated macrophage and suppresses gastric cancer growth

Next, we examined the function of lipid-induced macrophages with PI3K-γ inhibitor IPI-549. The phagocytic results showed that IPI-549 treatment leads to rescue of the inhibitory phagocytosis of macrophage (Figure 6E, F). There was no significant difference in the proliferation (Figure S5) or apoptosis (Figure S6) of tumor cells treated with IPI-549. Migration and invasive assays showed that the ablation of PI3K-γ counteracts the pro–migration or pro–invasion capacity of macrophages induced by TES or lipid mixtures (Figure 6G; Figure S7). This functional assay indicated that selective ablation of macrophage PI3K-γ can rescue the functional polarization of macrophages induced by lipid accumulation from tumors. Subsequently, we want to understand the in vivo function of PI3K-γ inhibitor in the MFC gastric cancer model. We found that the treatment of myeloid-enriched MFC tumors with IPI-549 significantly delayed tumor growth (Figure 6H-i; Figure S8A, B). Furthermore, the IPI-549 treatment educated macrophages to a less immunosuppressive phenotype, which correlates with increased $CD8^{+}IFN\text{-}\gamma^{+}$ functional T cells in MFC tumors (Figure S8C) and decreased lipid accumulation in TAM (Figure S8D). Taken together, these results demonstrate that TAM with high lipid content exhibit protumorigenic characteristics (Figure 7). These findings suggest that pharmacological normalization of lipid abundance in TAM with an inhibitor of PI3K-γ reduces the protumoral function of TAM, ultimately promoting T-cell-mediated cytotoxicity and inhibiting MFC tumor growth.

4 | DISCUSSION

Here we found that TAM are characterized by an increased amount of lipids in mice and humans. Functionally, TAM with a higher lipid content level display M2-like characteristics with decreased phagocytosis and enhanced anti–tumor immunity. Tumor-derived lipid content induce TAM polarization through the induction of PI3K-γ expression, and pharmaceutical targeting of PI3K-γ overcomes the protumor function of TAM to inhibit tumor growth of gastric cancer.

Recently, several studies have addressed the important role of lipids in immune cells, including dendritic cells and myeloid-derived suppressor cells (MDSC).[16,17,26,27] It has been shown that lipid accumulation driven by tumor-derived factors contributes to tumor-associated DC dysfunction in several cancers.[16,27,28] Similarly, MDSC took up the high lipid content, leading to profound metabolic and functional changes.[17] Here, we provide evidence that lipid accumulation also presents in TAM. Combined with our results, these accumulated reports have confirmed that myeloid cells can choose the metabolic programs allowing them to assemble their survival and functional demands under the conditions in the surrounding microenvironment.

Lipids accumulation in TAM has a profound effect on the functional polarization of macrophages with pro–tumor activity. Our observation supports the previous report that the uptake of triacylglycerols followed by lipolysis is critical for M2 polarized macrophage activation, and blockade of this process inhibits M2

macrophage function.[29] M2 macrophages rely on fatty acid oxidation to proliferate and support their function.[30,31] Moreover, higher lipid-laid TAM have reduced phagocytic potency against tumor cells and are not able to effectively stimulate allogeneic T cells. We replicated lipid accumulation of macrophages with tumor conditioned media and tumor explants, and the lipidomic profiling assay indicated that tumor-derived lipids were responsible for this phenomenon. Research has shown that there is an abundance of lipids in the tumor microenvironment that can be acquired by cancer cells or immune cells.[16,17,32] Raised serum lipid levels are present in gastric cancer patients and favor tumor progression.[33,34] Although our data support the increased lipid uptake in TAM from cancer cells, we cannot exclude the possibility of increased synthesis of fatty acids involved in lipid accumulation in TAM. Considering the significance of lipid-loaded accumulation in TAM for tumor progression, future work is necessary to further address these differences in the context of lipid accumulation of TAM.

Here, we demonstrated that the effect of lipid accumulation conferred the M2-like polarization of TAM with protumoral activity. Lipid-accumulated TAM upregulate PD-L1 expression, which blocks anti–tumor T cell responses to support their immunosuppressive functions. Therefore, exploring the mechanisms of lipid-laid TAM hold potential for the development of therapeutic interventions. The PI3K-AKT signaling pathway was the top pathway enriched in lipid-accumulated TAM. Consistently, previous works have shown that PI3K-γ is a molecular switch that controls the pro–tumor function of myeloid cells and promotes the production of inflammatory mediators and tumor migration.[35,36] PI3K-γ was induced in macrophages by lipid accumulation from tumor-derived lipids or exogenous lipid mixture. Interestingly, we also found reduced lipid accumulation in TAM from MFC-bearing mice after PI3K-γ inhibitor treatment, meaning the PI3K-γ pathway might contribute to the intrinsic lipid generation in TAM. Alternatively, the reduced lipid accumulation in TAM might be due to the dominant M1-like TAM after PI3K-γ inhibitor treatment. Pharmacological downregulation of PI3K-γ improves phagocytosis and antitumor responses in vitro and in vivo, which indicates that targeting of PI3K-γ signaling pathways in macrophages may provide a novel potential approach to improve the long-term survival of gastric cancer patients.

We found that lipid accumulation induced by tumor cell-derived lipids has an important role in the induction of TAM with pro–tumor activity. Given that targeting of the PI3K-γ signaling pathway overcomes the pro–tumor function of lipid-laid macrophages, a selective inhibitor of PI3K-γ is expected to be applied in clinical trials as a monotherapy or in combination with an immune checkpoint blockade for gastric cancer patients.

ACKNOWLEDGMENTS

We thank our colleagues in the department of laboratory medicine and the department of general surgery for helpful discussions and valuable assistance. This work was partly supported by the National Natural Science Foundation of China (No. 81772525, 81672363, 81402148, and 81472244).

DISCLOSURE

The authors have no conflict of interest.

ETHICAL CONSIDERATION

All studies were performed in accordance with the Declaration of Helsinki principals and the guidelines of the Research Ethics Committee of Xinhua hospital affiliated to Shanghai Jiao Tong University School of Medicine, and written informed consent was received from all patients.

ORCID

Lisong Shen https://orcid.org/0000-0002-6647-4749

REFERENCES

1. Chen W, Zheng R, Baade PD, et al. Cancer statistics in China, 2015. *CA Cancer J Clin*. 2016; 66:115-132.
2. Siegel RL, Miller KD, Jemal A. Cancer statistics, 2018. *CA Cancer J Clin*. 2018; 68:7-30.
3. Siegel RL, Miller KD, Jemal A. Cancer statistics, 2019. *CA Cancer J Clin*. 2019; 69:7-34.
4. Turley SJ, Cremasco V, Astarita JL. Immunological hallmarks of stromal cells in the tumour microenvironment. *Nat Rev Immunol*. 2015;15:669-682.
5. Pollard JW. Tumour-educated macrophages promote tumour progression and metastasis. *Nat Rev Cancer*. 2004;4:71-78.
6. Zhang J, Yan Y, Yang Y, et al. High infiltration of tumor-associated macrophages influences poor prognosis in human gastric cancer patients, associates with the phenomenon of EMT. *Medicine (Baltimore)*. 2016;95:e2636.
7. Zhang QW, Liu L, Gong CY, et al. Prognostic significance of tumor-associated macrophages in solid tumor: a meta-analysis of the literature. *PLoS One*. 2012;7:e50946.
8. Wang B, Xu D, Yu X, et al. Association of intra-tumoral infiltrating macrophages and regulatory T cells is an independent prognostic factor in gastric cancer after radical resection. *Ann Surg Oncol*. 2011;18:2585-2593.
9. Steidl C, Lee T, Shah SP, et al. Tumor-associated macrophages and survival in classic Hodgkin's lymphoma. *N Engl J Med*. 2010;362:875-885.
10. Gordon S. Alternative activation of macrophages. *Nat Rev Immunol*. 2003;3:23-35.
11. Murray PJ, Allen JE, Biswas SK, et al. Macrophage activation and polarization: nomenclature and experimental guidelines. *Immunity*. 2014;41:14-20.
12. Zhihua Y, Yulin T, Yibo W, et al. Hypoxia decreases macrophage glycolysis and M1 percentage by targeting microRNA-30c and mTOR in human gastric cancer. *Cancer Sci*. 2019;110:2368-2377.
13. Sica A, Schioppa T, Mantovani A, Allavena P. Tumour-associated macrophages are a distinct M2 polarised population promoting tumour progression: potential targets of anti–cancer therapy. *Eur J Cancer*. 2006;42:717-727.
14. Yamaguchi T, Fushida S, Yamamoto Y, et al. Tumor-associated macrophages of the M2 phenotype contribute to progression in gastric cancer with peritoneal dissemination. *Gastric Cancer*. 2016;19:1052-1065.
15. O'Neill LA, Pearce EJ. Immunometabolism governs dendritic cell and macrophage function. *J Exp Med*. 2016;213:15-23.
16. Herber DL, Cao W, Nefedova Y, et al. Lipid accumulation and dendritic cell dysfunction in cancer. *Nat Med*. 2010;16:880-886.
17. Al-Khami AA, Zheng L, Del Valle L, et al. Exogenous lipid uptake induces metabolic and functional reprogramming

of tumor-associated myeloid-derived suppressor cells. *Oncoimmunology*. 2017;6:e1344804.
18. Condamine T, Dominguez GA, Youn JI, et al. Lectin-type oxidized LDL receptor-1 distinguishes population of human polymorphonuclear myeloid-derived suppressor cells in cancer patients. *Sci Immunol*. 2016;1:aaf8943.
19. Xu W, Yu L, Zhou W, Luo M. Resistin increases lipid accumulation and CD36 expression in human macrophages. *Biochem Biophys Res Commun*. 2006;351:376-382.
20. Bobryshev YV, Ivanova EA, Chistiakov DA, Nikiforov NG, Orekhov AN. Macrophages and their role in atherosclerosis: pathophysiology and transcriptome analysis. *Biomed Res Int*. 2016;2016:9582430.
21. Zheng P, Chen L, Yuan X, et al. Exosomal transfer of tumor-associated macrophage-derived miR-21 confers cisplatin resistance in gastric cancer cells. *J Exp Clin cancer Res*. 2017;36:53.
22. Qiu B, Simon MC. BODIPY 493/503 staining of neutral lipid droplets for microscopy and quantification by flow cytometry. *Bio Protoc*. 2016;6:e1912.
23. Colegio OR, Chu NQ, Szabo AL, et al. Functional polarization of tumour-associated macrophages by tumour-derived lactic acid. *Nature*. 2014;513:559-563.
24. Kaneda MM, Messer KS, Ralainirina N, et al. PI3Kgamma is a molecular switch that controls immune suppression. *Nature*. 2016;539:437-442.
25. Santos-Sierra S, Deshmukh SD, Kalnitski J, et al. Mal connects TLR2 to PI3Kinase activation and phagocyte polarization. *EMBO J*. 2009;28:2018-2027.
26. Hossain F, Al-Khami AA, Wyczechowska D, et al. Inhibition of fatty acid oxidation modulates immunosuppressive functions of myeloid-derived suppressor cells and enhances cancer therapies. *Cancer Immunol Res*. 2015;3:1236-1247.
27. Gardner JK, Mamotte CD, Patel P, Yeoh TL, Jackaman C, Nelson DJ. Mesothelioma tumor cells modulate dendritic cell lipid content, phenotype and function. *PLoS One*. 2015;10:e0123563.
28. Ramakrishnan R, Tyurin VA, Veglia F, et al. Oxidized lipids block antigen cross-presentation by dendritic cells in cancer. *J Immunol*. 2014;192:2920-2931.
29. Huang SC, Everts B, Ivanova Y, et al. Cell-intrinsic lysosomal lipolysis is essential for alternative activation of macrophages. *Nat Immunol*. 2014;15:846-855.
30. Odegaard JI, Chawla A. Alternative macrophage activation and metabolism. *Annu Rev Pathol*. 2011;6:275-297.
31. Vats D, Mukundan L, Odegaard JI, et al. Oxidative metabolism and PGC-1beta attenuate macrophage-mediated inflammation. *Cell Metab*. 2006;4:13-24.
32. Ackerman D, Simon MC. Hypoxia, lipids, and cancer: surviving the harsh tumor microenvironment. *Trends Cell Biol*. 2014;24:472-478.
33. Kitayama J, Hatano K, Kaisaki S, Suzuki H, Fujii S, Nagawa H. Hyperlipidaemia is positively correlated with lymph node metastasis in men with early gastric cancer. *Br J Surg*. 2004;91:191-198.
34. Wulaningsih W, Garmo H, Holmberg L, et al. Serum lipids and the risk of gastrointestinal malignancies in the Swedish AMORIS Study. *J Cancer Epidemiol*. 2012;2012:792034.
35. Schmid MC, Avraamides CJ, Dippold HC, et al. Receptor tyrosine kinases and TLR/IL1Rs unexpectedly activate myeloid cell PI3kgamma, a single convergent point promoting tumor inflammation and progression. *Cancer Cell*. 2011;19:715-727.
36. Hirsch E, Katanaev VL, Garlanda C, et al. Central role for G protein-coupled phosphoinositide 3-kinase gamma in inflammation. *Science*. 2000;287:1049-1053.

SUPPORTING INFORMATION

Additional supporting information may be found online in the Supporting Information section.

How to cite this article: Luo Q, Zheng N, Jiang L, et al. Lipid accumulation in macrophages confers protumorigenic polarization and immunity in gastric cancer. *Cancer Sci*. 2020;111:4000–4011. https://doi.org/10.1111/cas.14616